Neuron, Vol. 16, 207–218, January, 1996, Copyright ©1996 by Cell Press

Transfer of 1,4-Dihydropyridine Sensitivity from L-Type to Class A (BI) Calcium Channels

Manfred Grabner, Zhengyi Wang, Steffen Hering, Jörg Striessnig, and Hartmut Glossmann
Institut für Biochemische Pharmakologie
Universität Innsbruck
Peter Mayrstraße 1
A-6020 Innsbruck
Austria

Summary

L-type Ca^{2+} channels are characterized by their unique sensitivity to organic Ca^{2+} channel modulators like the 1,4-dihydropyridines (DHPs). To identify molecular motifs mediating DHP sensitivity, we transferred this sensitivity from L-type Ca^{2+} channels to the DHP-insensitive class A brain Ca^{2+} channel, BI-2. Expression of chimeras revealed minimum sequence stretches conferring DHP sensitivity including segments IIIS5, IIIS6, and the connecting linker, as well as the IVS5–IVS6 linker plus segment IVS6. DHP agonist and antagonist effects are determined by different regions within the repeat IV motif. Sequence regions responsible for DHP sensitivity comprise only 9.4% of the overall primary structure of a DHP-sensitive α_{1A}/α_{1S} construct. This chimera fully exhibits the DHP sensitivity of channels formed by L-type α_1 subunits. In addition, it displays the electrophysiological properties of α_{1A}, as well as its sensitivity toward the peptide toxins ω-agatoxin IVA and ω-conotoxin MVIIC.

Introduction

In excitable cells, intracellular concentrations of free Ca^{2+} are regulated via voltage-dependent Ca^{2+} channels. These channels can be distinguished according to biophysical and pharmacological criteria into different types (L, P, N, R, Q, and T; Birnbaumer et al., 1994; Dunlap et al., 1995). At least three classes of α_1 subunits, encoded by different genes, participate in the formation of L-type channels: class S in skeletal muscle; class C in smooth muscle, cardiac muscle, and neurons; and class D in neuroendocrine cells (reviewed in Hofmann et al., 1994). They can be discriminated from all other Ca^{2+} channel types by their sensitivity to 1,4-dihydropyridines (DHPs). These drugs label a high affinity DHP receptor domain located on the channel's α_1 subunit (Catterall et al., 1988; Glossmann and Striessnig, 1990). Some DHPs act as ''Ca^{2+} antagonists'' or channel blockers (e.g., isradipine, nifedipine, nimodipine), preferentially stabilizing the inactivated state of the channel, whereas others (e.g., Bay K 8644) are ''Ca^{2+} agonists'' (channel activators) and promote the open state (Hess, 1990; Hille, 1992).

To gain a deeper insight into the molecular mechanism of L-type channel modulation by DHPs, attempts were made to elucidate the structural details of the DHP binding domain(s). With peptide mapping techniques after photolabeling, two distant sequence stretches were found to contribute to the formation of the DHP receptor site on the α_{1S} subunit (Nakayama et al., 1991; Striessnig et al., 1991; Catterall and Striessnig, 1992). These comprised parts of the pore-lining S5-S6 linkers (P or SS regions) together with transmembrane segments S6 of repeats III (IIIS6) and IV (IVS6). Together with electrophysiological studies (Kass and Arena, 1989; Kass et al., 1991; Strübing et al., 1993), these data provided evidence that regions close to segment IIIS6 and near the extracellular pore opening form the core of the DHP receptor site.

In the first approach with recombinant DNA-techniques to localize regions critical for DHP action, chimeric α_1 constructs were analyzed after functional expression (Tang et al., 1993). The DHP sensitivity of the α_{1C} subunit (Mikami et al., 1989) was lost after specific insertions of corresponding parts of a DHP-insensitive α_{1A} subunit (Mori et al., 1991). In agreement with earlier results from peptide mapping experiments (Nakayama et al., 1991; Striessnig et al., 1991; Catterall and Striessnig, 1992), it was concluded that the C-terminal half of repeat IV of α_{1C} must contain regions necessary for sensitivity to DHPs. A role of the SS2-S6 region of repeat III for DHP action was strongly rejected by Tang et al. (1993). However, this conclusion was based on experiments in which only a portion of the proposed core region of the DHP receptor site was replaced by the α_{1A} sequence.

We have now identified in great detail the sequence stretches within various α_1 subunits that confer DHP drug sensitivity. In contrast to a ''destructive'' approach (i.e., removal of drug sensitivity via chimeric constructs), we favored a ''constructive'' method. Here, we transposed sequence stretches from two distinct classes of DHP-sensitive L-type channel α_1 subunits, namely from rabbit heart α_{1C} (Mikami et al., 1989) and carp (Cyprinus carpio) skeletal muscle α_{1S} (Grabner et al., 1991) into the corresponding regions of the DHP-insensitive rabbit brain α_{1A} (BI-2) channel (Mori et al., 1991). Chimeric channels were studied for DHP agonist and antagonist sensitivity after heterologous expression in Xenopus laevis oocytes. Our final goal was to create a DHP agonist– and DHP antagonist–sensitive α_1 chimeric construct containing only a minimal quantity of L-type sequence (''minimum chimera'').

Our results demonstrate that 9.4% of L-type α_1 sequence, covering transmembrane segments IIIS5 and IIIS6, including their connecting linker (pore loop), together with a second motif comprising the IVS5-IVS6 linker plus transmembrane segment IVS6, are sufficient to introduce DHP agonist and antagonist sensitivity into α_{1A}. Biophysical and pharmacological properties of this minimum chimera were studied and compared with channels entirely composed of L-type sequence. Subsequently, we identified distinct regions responsible for agonist or antagonist action within these ''minimum motifs.'' Delineating the architecture of the DHP-agonist and DHP-antagonist interaction sites on the level of individual amino acids now seems possible.

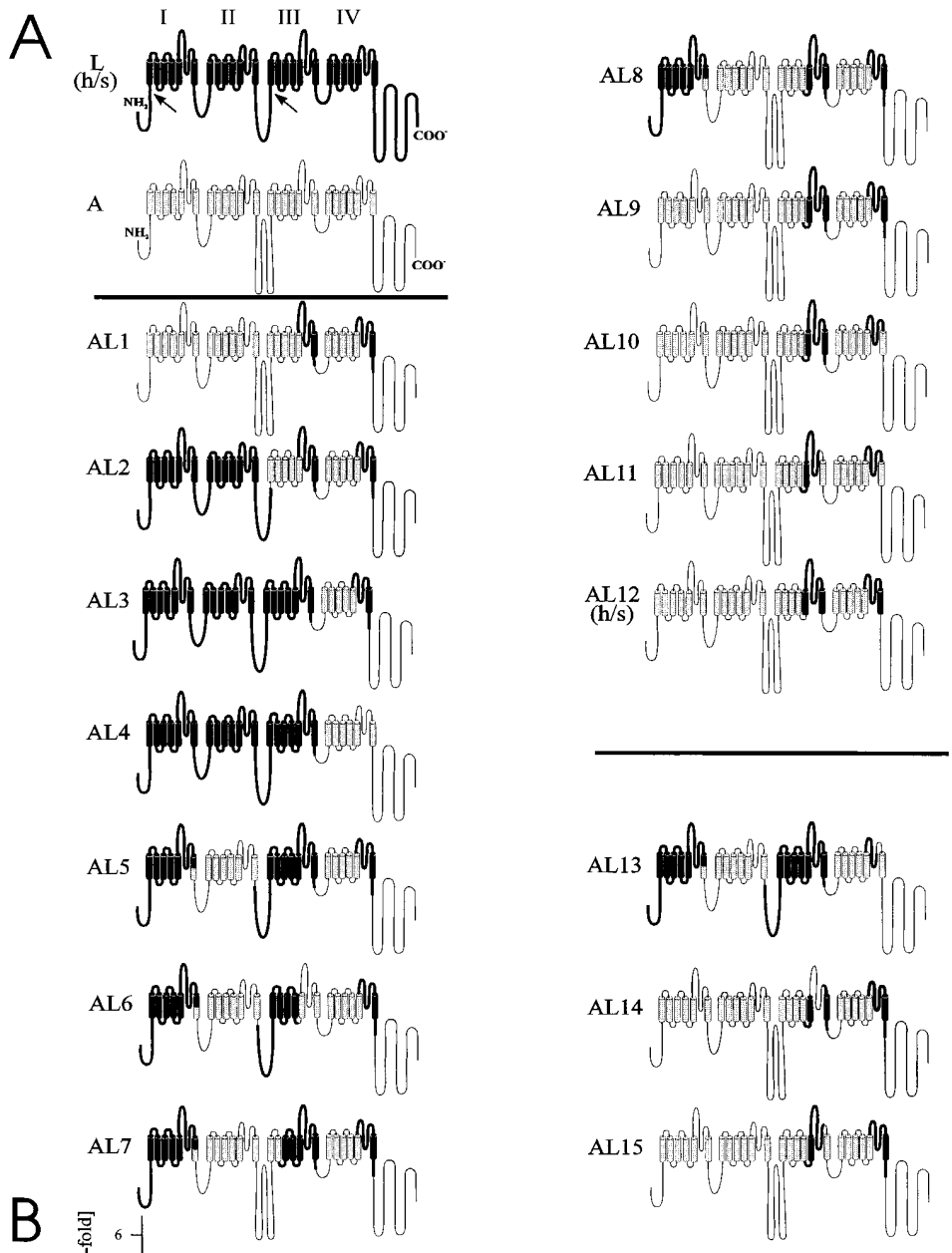
A
I
II
III
IV
L (h/s)
A
NH2
COO-
AL1
AL2
AL3
AL4
AL5
AL6
AL7
AL8
AL9
AL10
AL11
AL12 (h/s)
AL13
AL14
AL15
B
IBa Increase by (+)BAY K 8644 (10µM) [-fold]
IBa Block by (+)Isradipine (10µM) [%]
Lh Ls A 1 2 3 4 5 6 7 8 9 10 11 12h 12s 13 14 15

Results

Mapping the Sequence Motifs Responsible for DHP Sensitivity of L-Type α_1 Subunits

To determine the regions mediating DHP sensitivity in L-type calcium channels, we introduced sequence stretches from two different DHP-sensitive L-type channel α_1 subunits into the DHP-insensitive α_{1A} (Mori et al., 1991). All chimeras were coexpressed in X. laevis oocytes, together with the β_{1A} subunit. Ca^{2+} channel β subunits are known to enhance channel function (current amplitudes, drug binding) and also to affect current kinetics (Lacerda et al., 1991; Mori et al., 1991; Varadi et al., 1991; Wei et al., 1991; Grabner et al., 1994; Mitterdorfer et al., 1994). Figure 1A gives a schematic structural overview and Figure 1B, an overview on the sensitivity of the resulting chimeras toward DHP agonists and antagonists, respectively. The DHP-sensitive α_1 subunits used for chimerization were α_{1C} from rabbit heart (Mikami et al., 1989) and α_{1S} from carp skeletal muscle (Grabner et al., 1991). Similar to α_{1S} from rabbit skeletal muscle (Tanabe et al., 1987), α_{1S} from carp skeletal muscle could not be functionally expressed in Xenopus oocytes. However, after replacing repeats I and II of carp α_{1S} with the corresponding α_{1C} sequences, this construct (termed Ls in Figure 1A) formed DHP agonist– and DHP antagonist–sensitive channels (Figure 1B and Figure 2). In contrast, a construct (data not shown) that contained repeats I and II from α_{1C} and repeats III and IV from α_{1A} remained DHP insensitive like α_{1A}. Clearly, repeats I and II alone do not determine DHP sensitivity, but repeats III and IV of carp α_{1S} supported DHP sensitivity and could therefore be for used for chimerization. As previously described (Wang et al., 1995) the expression of α_{1C} was improved by replacing parts of its N-terminus with carp α_{1S} sequence. The respective construct is termed Lh. Also, chimera Ls contained the carp α_{1S} N-terminal sequence.

Figure 2 illustrates electrophysiological properties and DHP sensitivity of Lh (Figure 2A), Ls (Figure 2B), and α_{1A} (Figure 2C). Ls activated significantly more slowly than the other constructs. A detailed comparison of the kinetic properties of Lh and Ls has been published recently (Wang et al., 1995). In contrast to the other constructs, Ba^{2+} inward currents (I_{Ba}) through α_{1A} showed significant inactivation of typically 35%–50% of the current after a 350 ms test pulse to +10 mV. Inward currents through α_{1A} were unaffected by 10 μM solutions of (±)-Bay K 8644 and (±)-isradipine (Figure 2C).

I_{Ba} of chimeras Lh and Ls were stimulated by the DHP agonist (±)-Bay K 8644 (10 μM) and blocked by (±)-isradipine (10 μM; Figure 2). As observed with native L-type channels, Bay K 8644 increased peak I_{Ba}; slowed current activation; shifted the peak, as well as the midpoint voltage of the current activation curve to more negative potentials; and slowed tail currents (Figure 2). Current block by the DHP antagonist (±)-isradipine (10 μM) was accompanied by an acceleration of current decay (Figure 2) and a shift of the steady-state inactivation curve toward more negative voltages (data not shown). Despite the pronounced differences in current kinetics between Lh and Ls, similar changes in the voltage-dependence of I_{Ba} were induced by Bay K 8644. The observed shift in the voltage dependence of activation to negative potentials was, however, less pronounced for chimera Ls (Figures 2A and 2B).

The effect of the antagonist isradipine on I_{Ba} inactivation was most prominent for the slowly activating chimera Ls. Under control conditions, current did not reach its peak during a 350 ms test pulse (Figure 2B) (see also Wang et al., 1995) but ''inactivated'' in the presence of 10 μM (±)-isradipine (Figure 2B). Therefore, these isradipine induced changes in current kinetics, especially of the slowly activating chimeras, precluded a comparison of the drug effects (Figure 1B) by measuring inhibition of peak current values. Antagonist effects of isradipine were therefore evaluated as current inhibition at the end of a 350 ms test pulse to +20 mV. Taking into account that the agonist effects on I_{Ba} were always more pronounced in the voltage range from −10 to 0 mV, we assessed DHP agonist effects on I_{Ba} as the increase in maximum current amplitude during a 350 ms test pulse to −10 to 0 mV (Figure 1B).

Previous work suggested that the pore regions and adjacent transmembrane segments S6 of repeats III and IV of skeletal muscle α_{1S} play a key role for the formation of the DHP receptor site (Nakayama et al., 1991; Striessnig et al., 1991; Tang et al., 1993). Consequently, chimera AL1 (Figure 1A) was constructed where these regions were replaced in α_{1A} by the corresponding carp α_{1S} L-type sequences. AL1 displayed kinetic properties typical for α_{1A} (Mori et al., 1991; Sather et al., 1993) but surprisingly was insensitive to 10 μM of the DHP agonist (±)-Bay K 8644 or the antagonist (±)-isradipine (Figure 1B). Clearly, additional regions are required to mediate DHP sensitivity. As for α_{1A} (see above), replacement of repeats I and II by α_{1C} sequence in AL2 (Figure 1A) did not support DHP sensitivity (Figure 1B). Therefore, a model is unlikely where all four P regions form a (pseudo) symmetrical interaction site. DHP-agonist and DHP-antagonist sensitivity could be restored by changing the

Figure 1. Contribution of Individual Regions of α_1 Subunits to DHP Sensitivity

(A) Schematic representation of the DHP-insensitive class A channel (designated: A) and of the chimeric α_1 subunits L and AL1–AL15. DHP-sensitive L-type sequence stretches are indicated by black segments and bold lines. Gray segments and thin lines represent DHP-insensitive α_{1A} sequences. Arrows indicate the transitions between the different L-type sequence stretches (see Results and Experimental Procedures) in chimeras Lh and Ls.

(B) Inhibition or stimulation of barium currents (I_{Ba}) through chimeric channels expressed in oocytes of X. laevis, elicited by 10 μM solutions of racemic isradipine and Bay K 8644, respectively. Chimeras AL1–AL15 are indicated by numbers 1–15, respectively. Bars represent the mean ± SEM of 4 to 11 experiments in oocytes from at least 2 frogs. Block (current inhibition at the end of a 350 ms test pulse to a test potential of +20 mV) and stimulation of I_{Ba} (increase of maximal current amplitude during a 350 ms depolarization to a test potential 20 mV negative to the peak potential of the I–V curve) were recorded in 40 mM Ba^{2+} from a holding potential of −80 mV.

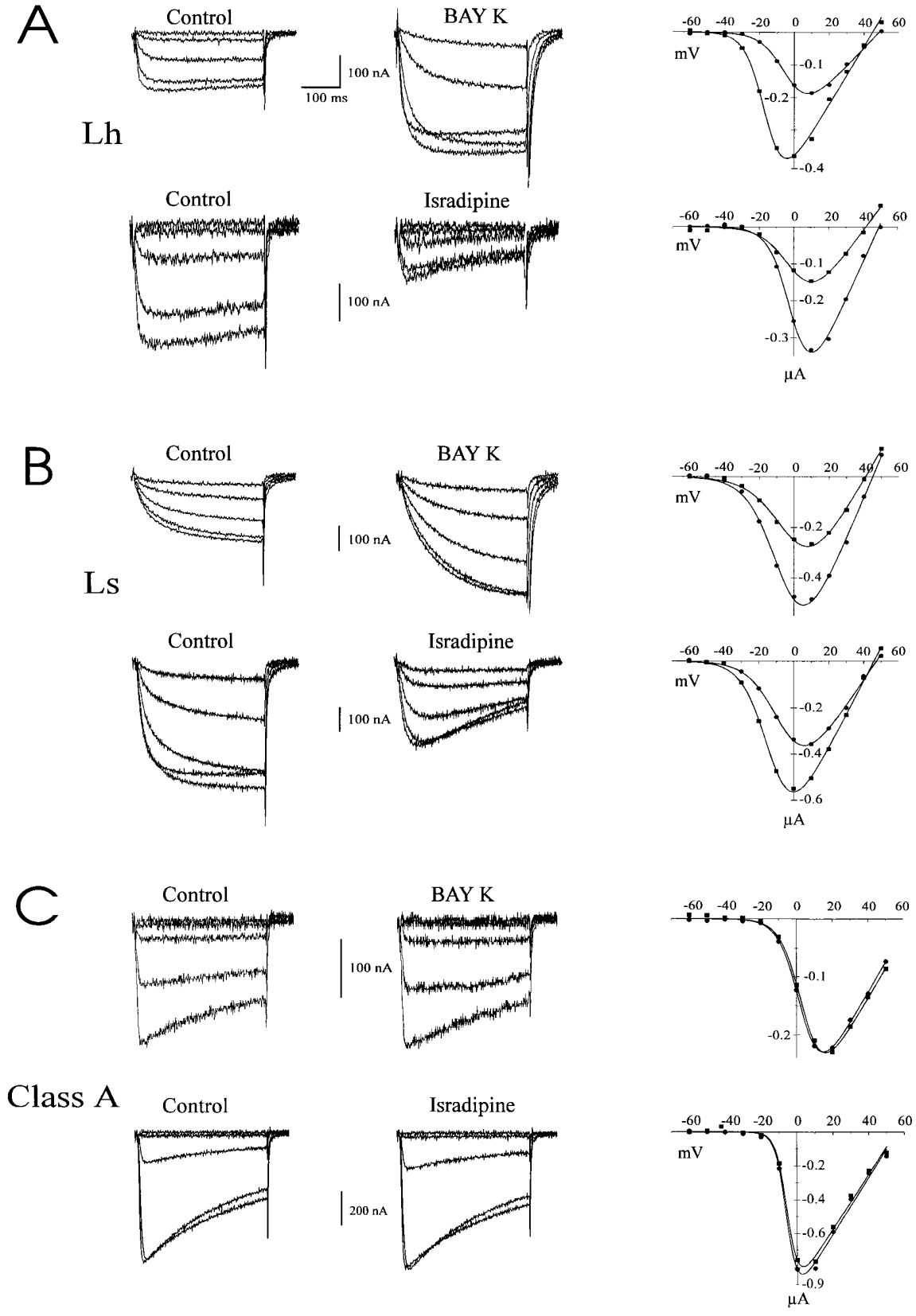

Figure 2. Effects of DHPs on I_{Ba} Carried by L-type Chimeras Lh and Ls or by the Class A Channel α_{1A}

(Left column) Families of I_{Ba} currents shown for L-type chimeras Lh (A) and Ls (B) and for α_{1A} (C) were recorded in 10 mV increments at test potentials ranging from −30 to +20 mV from a holding potential of −80 mV. Currents had threshold potentials in the range of −40 to −20

region from segment IIIS1 through IIIS5 of AL2 from class A to L-type sequence yielding chimera AL3 (Figure 1). This suggested an essential role of IIIS1-IIIS5 (or at least parts of it) for DHP action. Moreover, restoration of DHP sensitivity in chimera AL3 also indicated that the carboxy-terminal tail of the α_1 subunit has no essential role in the formation of the DHP binding pocket.

After replacement of the IVS5-IVS6 linker plus segment IVS6 of AL3 by class A sequence to create chimera AL4, the DHP agonist and antagonist sensitivity was removed (Figure 1B), which in accordance with the results of previous peptide mapping and chimeric deletion studies (Nakayama et al., 1991; Striessnig et al., 1991; Tang et al., 1993) confirms that this part of repeat IV is an essential element for DHP interaction.

In chimera AL5, repeat II, the I-II linker, and the C-terminal half of IS6 of chimera AL3 were replaced by α_{1A} sequence (Figure 1A). As DHP sensitivity was fully preserved in AL5 (Figure 1B), the sequence divergence between L-type and class A channels within this region does not account for the differences in DHP sensitivity. Unfortunately, at this point we were unable to test the importance of repeat I, as the expression of chimeras composed of repeat I from α_{1A} and repeat III from α_{1S} did not yield functional channels. This result was obtained with several independent polymerase chain reaction (PCR) products. It could not be explained by PCR-induced changes in the DNA sequence as confirmed by DNA sequencing of PCR-generated repeat I cDNAs.

As a next step, we further reduced the amount of L-type sequence of repeat III starting from chimera AL5. Evidence for an important role of segments IIIS5 and IIIS6 and the IIIS5-IIIS6 linker was demonstrated by the loss of DHP sensitivity in AL6, where the stretch from IIIS5-IIIS6 was switched to class A sequence. Because L-type sequence only within the P region and S6 in repeat III, but excluding IIIS5, was not sufficient to create DHP sensitivity in chimeras AL1 and AL2, the results with AL6 suggest the importance of IIIS5. By constructing further chimeras (AL7 and AL8), we could exclude the following sequence stretches as contributing to DHP site formation: the cytoplasmic linker between repeats II and III, the region from segments IIIS1 to IIIS2 (chimera AL7), and the region from IIIS3 to IIIS4 (chimera AL8). After L-type sequences in repeat III were significantly reduced in chimera AL8, the swapping of repeat I from L-type to class A sequence was tolerated, yielding chimera AL9, which formed DHP-sensitive channels. AL9 was then further modified to refine the roles of transmembrane segments IVS6 and IIIS6 and of the remaining cytoplasmic sequences. Changing segments IVS6 of AL9 into class A sequence (chimera AL10) resulted in the complete loss of sensitivity for the DHP agonist Bay K 8644, whereas the sensitivity for the antagonist isradipine was retained. Similarly the antagonist- (but not agonist-) sensitive chimera AL13 demonstrates that L-type sequence is required only within a fraction of the IVS5-IVS6 linker to mediate antagonist sensitivity. These results extend the findings of Tang et al. (1993), as we can show that in repeat IV only sequence differences within IVS6 account for agonist sensitivity, whereas the N-terminal half of the IVS5-IVS6 linker of carp α_{1S} contributes also to DHP antagonist sensitivity.

To further refine the role of repeat III, we swapped segment IIIS6 from L-type to class A sequence (chimera AL11). This eliminated DHP antagonist and agonist sensitivity. Tang et al. (1993) replaced the first 9 amino acids of transmembrane segment IIIS6 in α_{1C} with α_{1A} sequence without detectable effect on DHP sensitivity (their chimera CBC3). As we completely replaced IIIS6, the amino acids responsible for DHP sensitivity have to be grouped between residues in positions 10–25 in IIIS6 of the corresponding α_{1C} sequence. All of the remaining intracellular sequences could be removed from chimera AL9 without loss of DHP sensitivity resulting in our minimum chimera, AL12s. The sensitivity of AL12 chimeras to (±)-Bay K 8644 and (±)-isradipine was preserved, irrespective of the source of L-type sequence used (α_{1C}, α_{1S}; yielding AL12h and AL12s, respectively; Figures 1A and 1B). Further replacement of L-type sequence within the P region as well as S6 in repeat III (see chimeras AL14 and AL15) yielded DHP agonist– and DHP antagonist–insensitive channels (Figure 1), demonstrating the importance of these regions for the formation of the DHP interaction site.

Properties of the Minimal Chimera AL12s

Of the AL12 construct sequences, 90% comprise α_{1A} sequence. The current kinetics of the studied chimeras closely resemble those of α_{1A} (Figure 1A and Figure 3); but, in contrast, the currents are sensitive to DHPs as exemplified for AL12s in Figures 3A–3F. Current increase by (±)-Bay K 8644 (Figure 3A) or by DHP agonist (+)-202–791 (Figure 3E) is associated with the typical shifts in the maximum of the I–V curves toward more negative potentials and similar changes in current kinetics as found for chimeras Lh and Ls (see Figure 2). Current inhibition by isradipine was concentration dependent and stereoselective (Figures 3C and 3D) and occurred with similar apparent potency as block of currents mediated by α_{1C} (Figure 3D). We found no evidence for major differences in DHP sensitivity between AL12s and α_{1C} (Figure 3D).

FPL 64176 is a novel benzoyl pyrrole L-type channel agonist structurally unrelated to DHPs. Radioligand binding studies indicate (Kunze and Rampe, 1992; Ginap et al., 1993) that FPL 64176 labels a site distinct from DHPs. Interestingly, FPL 64176 sensitivity is absent in α_{1A} (data not shown; but see Sather et al., 1993) but was introduced into chimera AL12s (Figure 3G). This suggests that critical determinants of the FPL 64176

mV and reached peak current values between 0 and +20 mV. One typical recording out of at least seven experiments is shown.
(Middle column) I_{Ba} recorded from the same oocytes 2–3 min after perfusion with solutions containing 10 μM of agonist (±)-Bay K 8644 or of antagonist (±)-isradipine.
(Right column) Corresponding current–voltage relations of maximum inward I_{Ba} obtained during 350 ms voltage steps before (squares) and after (circles) the application of DHPs. The holding potential was −80 mV, and test potentials ranged from −60 to +50 mV. The range of current stimulation by (±)-Bay K 8644 was as follows: Lh: 2.7- to 6.3-fold (n = 5); Ls: 1.7- to 7.5-fold (n = 7).

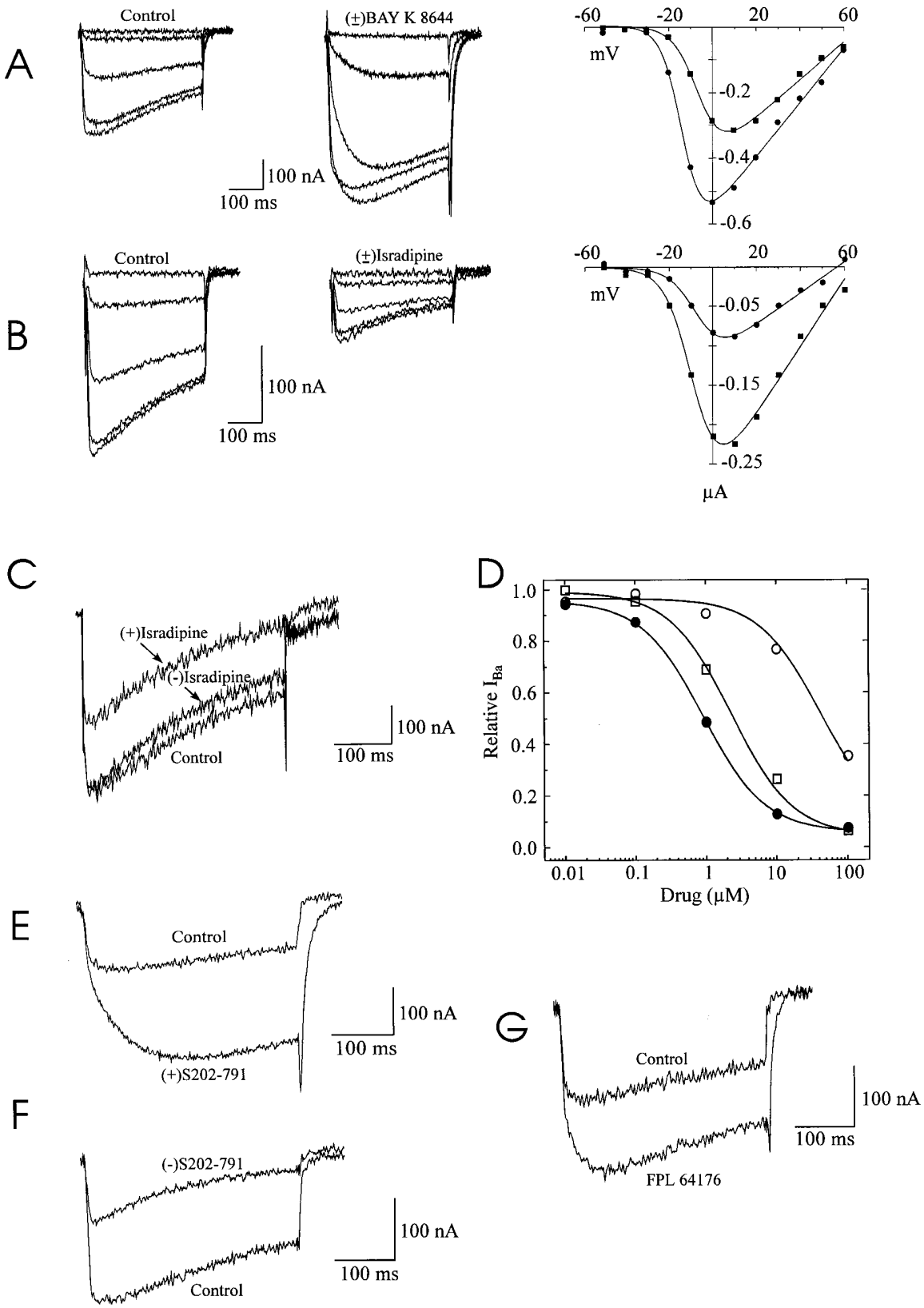

Figure 3. Electrophysiological and Pharmacological Properties of Chimera AL12s

In each panel typical recordings out of at least three experiments are shown.

(A and B) Families of currents recorded in 40 mM Ba^{2+} at test potentials from −30 to +10 mV from a holding potential of −80 mV are shown

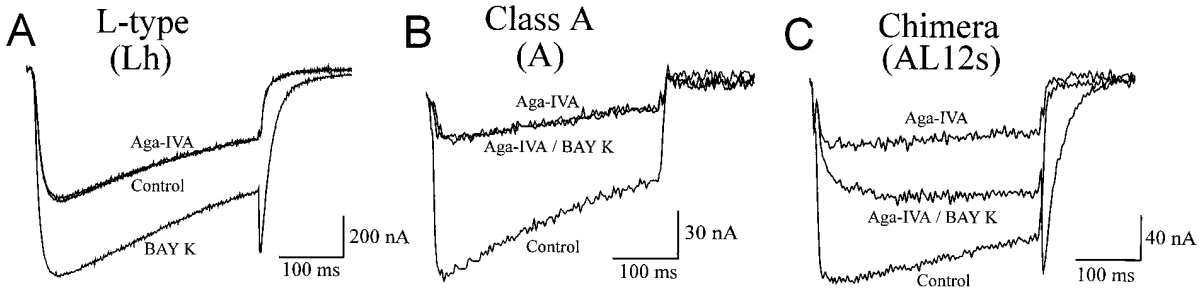

Figure 4. Sensitivity of Chimera AL12s to the Funnel Web Spider Toxin ω-Agatoxin-IVA

Experiments were carried out in 2 mM Ba^{2+} (low Ba^{2+} solution; test potential: −10 mV; holding potential: −80 mV). After recording the control I_{Ba}, oocytes were superfused with 1 μM of toxin-containing solution. After steady-state inhibition of I_{Ba} by the toxin had occurred (between 3 to 4 min), (±)-Bay K 8644 was added to 10 μM. Agonist-stimulated I_{Ba} was recorded 1 min after drug application. One out of three experiments yielding similar results is shown for Lh (A), α_{1A} (B), and AL12s (C).

and DHP binding domain are located in close vicinity within the α_1 subunit.

Neurotoxin Sensitivity of Chimera AL12s

Class A α_1 subunits expressed in Xenopus oocytes give rise to Q-type currents, similar to those recently described in hippocampal pyramidal and cerebellar granule neurons (Wheeler et al., 1994; Randall and Tsien, 1995). Q-type currents in Xenopus oocytes are blocked by the spider toxin ω-Agatoxin IVA (ω-Aga IVA; IC_{50} = 200–1000 nM; Sather et al., 1993; Stea et al., 1994) and by the marine snail toxin ω-conotoxin MVIIC (ω-CTx MVIIC; $IC_{50} > 100$ nM; Sather et al., 1993). Introduction of L-type sequence into α_{1A} (chimera AL12s) did not affect the sensitivity to these toxins. Block of AL12s by the two toxins was similar to the block observed for α_{1A} and is exemplified for ω-Aga-IVA in Figures 4B and 4C. As expected (Sather et al., 1993), α_{1C} (expressed as Lh) was toxin insensitive (Figure 4A). Similar to the ω-conotoxin GVIA block of N-type channels (Ellinor et al., 1994), these peptide toxins most likely interact with the channel at the outer entrance of the ionic pore. We therefore consider the two pore-forming linkers of α_{1A}, which were replaced by L-type sequences in AL12s to create the DHP sensitivity, as insignificant for toxin interaction.

Discussion

α_1 Subunit Regions Responsible for DHP Sensitivity

By generating a variety of chimeric α_1 constructs between DHP-sensitive and DHP-insensitive α_1 subunits, we succeeded in introducing DHP sensitivity into the a priori DHP-insensitive α_{1A} subunit. L-type sequence stretches required for transfer of DHP sensitivity were associated exclusively with repeats III and IV. The DHP agonist– and DHP antagonist–sensitive chimeras with minimum L-type sequence portions contained L-type sequences of either α_{1C} or carp α_{1S} in transmembrane segments IIIS5, IIIS6, and IVS6, as well as in the S5-S6 linkers in repeats III and IV. Combining results of the present work with previous data (Tang et al., 1993) leads to a model of minimal L-type sequence requirements for the formation of the DHP binding pocket as depicted in Figures 5A and 5B. According to a molecular model of voltage gated cation channels (Guy and Conti, 1990) these sequence stretches are believed to participate directly in the formation of the ion conducting pathway or to be located close to the extracellular pore opening (Figure 5C). A further reduction of L-type sequence in repeat III resulted in a loss of DHP effects, suggesting that structural determinants for both DHP agonist and antagonist interaction reside close to pore-forming regions in repeat III. The second DHP interaction site formed by residues in repeat IV is able to discriminate between channel activators and blockers: critical determinants for DHP agonists are located within transmembrane segment IVS6 of L-type channels, whereas L-type-channel-specific residues support DHP antagonist action within the N-terminal half of the IVS5-IVS6 linker. Functional studies have provided evidence for distinct DHP agonist and antagonist interaction sites (Kamp et al., 1989; Lacerda and Brown, 1989; Hughes et al., 1990). DHPs induce a variety of changes in Ca^{2+} channel gating and different channel state models have been proposed to explain kinetic effects on single channel and whole cell Ca^{2+} channel currents (Bean, 1984; Hess et al., 1984; Sanguinetti et al., 1986; Hering et al.,

before (left panel) and after (middle panel) application of 10 μM (±)-Bay K 8644 (A) or (±)-isradipine (B). The corresponding current–voltage relation curves (peak I_{Ba}) before (squares) and during (circles) drug application are shown at right.

(C) Stereoselective inhibition of I_{Ba} through chimera AL12s 3–4 min after perfusion with 1 μM (+)- and (-)-isradipine-containing solutions.

(D) Concentration–response curves of (+)-isradipine (closed circles) and (−)-isradipine (open circles) for inhibition of peak I_{Ba} carried by chimera AL12s, compared with the effects of (±)-isradipine on L-type chimera Lh (open squares). Data from three recordings were pooled and are given as means (SEM < 20%). IC_{50} values were calculated by fitting the experimental data to the general-dose-response equation (slope factor = 1; De Lean et al., 1978): Lh ([±]-isradipine): IC_{50} = 1.6 μM; AL12s ([+]-isradipine): IC_{50} = 910 nM; AL12s ([−]-isradipine): IC_{50} = 45 μM.

(E–G) Sensitivity of chimera AL12s to 10 μM solutions of the DHP agonist (+)-S202–791 (E), the DHP antagonist (−)S202–791 (F), and the non-DHP agonist FPL 64176 (G). (E)–(G) show representative current traces recorded during depolarization to a test potential of +10 mV from a holding potential of −80 mV.

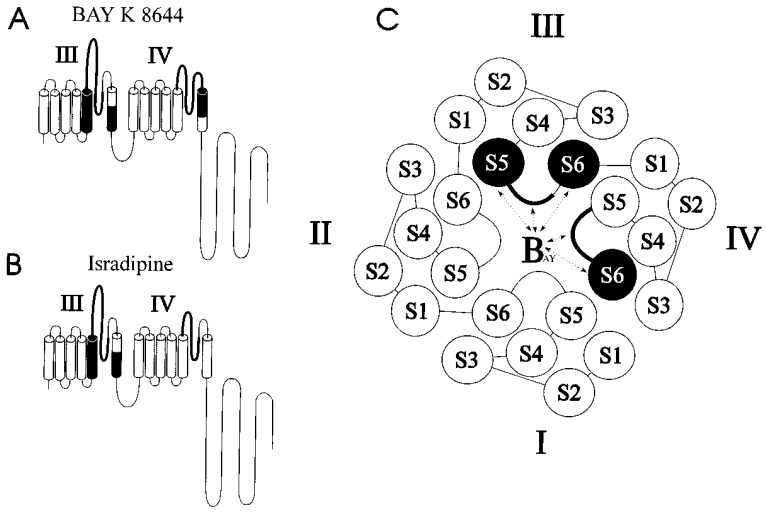

Figure 5. Proposed Minimum L-type Sequence Stretches Required for Making Class A Channel α_{1A} DHP Sensitive

Membrane folding model of the α_1 subunit depicting minimum L-type sequence requirements in DHP-insensitive class A channels for providing DHP-agonist (Bay K 8644) (A) and DHP-antagonist (isradipine) (B) sensitivity. Black segments and bold lines represent DHP-sensitive L-type sequence stretches; gray segments and thin lines, DHP-insensitive α_{1A} sequence stretches. As repeats I and II are entirely composed of α_{1A} sequence, only repeats III and IV are illustrated in (A) and (B). (C) Top view model of the α_1 subunit according to proposed molecular models (Guy and Conti, 1990). Circles symbolize transmembrane segments IS1–IVS6. Black circles and bold lines represent L-type channel sequences; gray circles and thin lines, class A. Proposed DHP agonist Bay K 8644 (''BAY'') interaction with structural elements of the α_1 subunit inside the channel pore is indicated by dotted lines and arrows.

1989; Lacerda and Brown, 1989; Marks and Jones, 1992; Bechem and Hoffmann, 1993). The contribution of distant portions of primary structure for the formation of a drug binding site may facilitate ''allosteric'' effects on L-type channel function, promoting closed (antagonist) or open (agonist) channel conformations. Such allosteric effects may be most easily exerted by interaction at the interface of protein subunits, as has been shown for allosteric enzymes (Sprang et al., 1987; Georgiadis et al., 1992). As the homologous repeats I–IV of the α_1 subunit can be regarded as individual channel subunits connected by cytoplasmic loops, DHP binding involving repeats III and IV may promote conformational changes of tertiary structure more efficiently than by interaction within only one repeat. It is, however, interesting to note that the typical changes in current kinetics produced by agonist and antagonist DHPs require structural elements that are localized in channel repeats III and IV, whereas molecular determinants for activation and inactivation have been localized in repeat I of the α_1 subunit (Tanabe et al., 1991; Nakai et al., 1994; Zhang et al., 1994; but see Wang et al., 1995).

In the present work, we extend previous findings concerning the localization of the DHP receptor domain obtained with antibody mapping (Nakayama et al., 1991; Striessnig et al., 1991) or chimeric constructs (Tang et al., 1993). First, our data provide—by a constructive chimeric approach—direct evidence for the involvement of residues within repeat III for DHP agonist and antagonist sensitivity. Second, we directly demonstrate that portions of the IVS5-IVS6 linker mediate DHP antagonist sensitivity. Third, our results show that receptors not only for peptide toxins (Gross et al., 1994) but also for small nonpeptidergic drugs can be successfully transferred between related ion channels. Obviously, the remaining ~90% of α_{1A} sequence of AL12s induces no steric distortion to the overall folding structure of a stereoselective DHP binding pocket. On the other hand, because the α_{1A}-specific sensitivity for peptide toxins was not impaired, the introduction of the DHP binding pocket seems not to interfere with the toxin interaction site(s). However, we cannot rule out slight changes in the DHP affinity of the recombinant DHP receptor site in our AL12 chimeras unresolved by functional expression in Xenopus oocytes. Fourth, by constructing chimeras Ls and AL12s, we provide evidence that the previously cloned α_1 subunit from carp (Cyprinus carpio) skeletal muscle belongs to the DHP-sensitive family of α_1 subunits—something that had not been directly supported by functional expression studies.

We conclude that the most important structural determinants for DHP sensitivity reside within the transposed L-type sequence stretches of chimeras AL12. However, we cannot completely exclude the possibility that, when bound to the channel with high affinity, the DHP molecule interacts with additional amino acids outside these regions that are also provided by the α_{1A} primary structure. For several reasons the identification of such residues will be difficult. One possible approach consists in the construction of chimeras analogous to AL12 but using a different DHP-insensitive α_1 subunit (e.g., α_{1B}) as a host sequence. The high sequence homology among non-L-type α_1 subunits is the main drawback for this approach. Alternatively, alanine scanning mutagenesis (Ragsdale et al., 1994) can be carried out but would require systematic mutation of a large number of residues.

Repeat III Participates in the Formation of the DHP Binding Pocket

Closer inspection of the sequence within the regions conferring DHP sensitivity to AL12 chimeras (Figure 6) revealed an overall sequence identity of 62% between α_{1C} and carp α_{1S}. The amino acid identities between these α_1 subunits and α_{1A} were 46% and 41%, respectively. A sequence alignment of the respective sequences is depicted in Figure 6. All amino acid residues within the α_{1A} sequence that were not conserved in one of both DHP-sensitive α_1 subunits used in our study are highlighted. Among those, asterisks indicate residues that

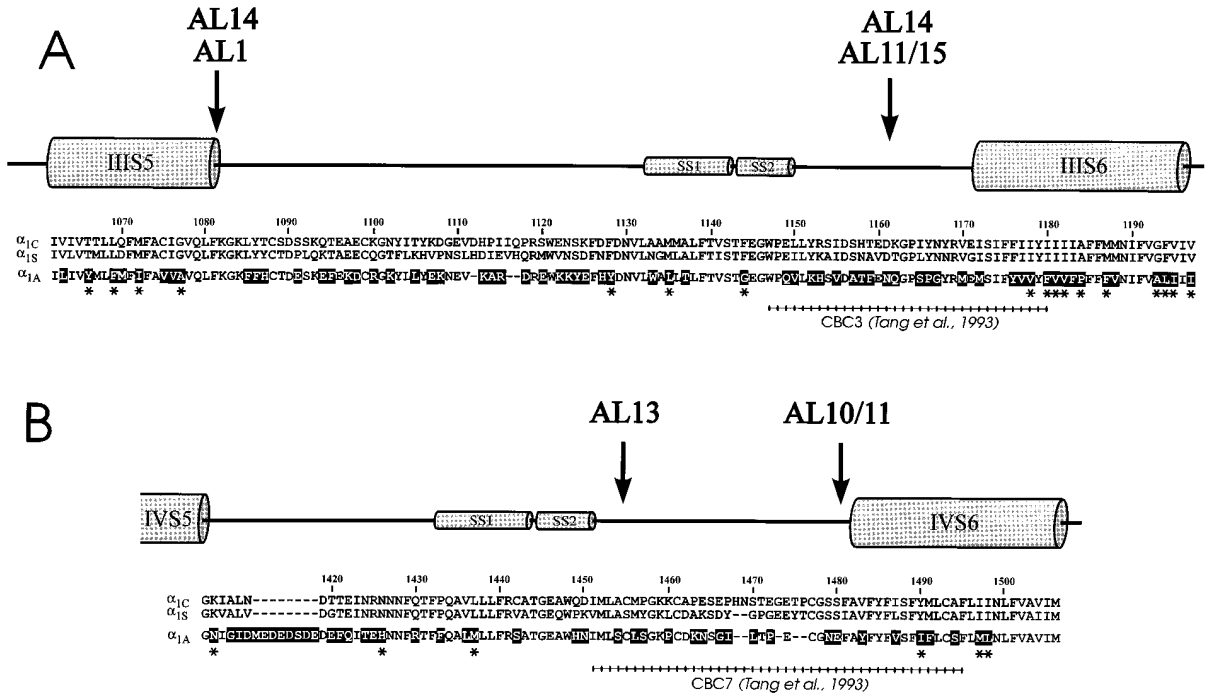

Figure 6. Partial Sequence Alignment of α_{1C} and Carp α_{1S} with the Corresponding α_{1A} Sequences

Amino acid alignment of sequence stretches of α_{1C} and carp α_{1S} of repeat III (A) and repeat IV (B) able to transfer DHP sensitivity into class A channels after replacing the aligned α_{1A} sequences (chimeras AL12). Transmembrane segments and intramembrane SS1-SS2 regions are indicated by cylinders. Numbers of amino acid positions correspond to α_{1C} (Mikami et al., 1989). Marked sequence stretches CBC3 and CBC7 refer to the chimeric constructs analyzed by Tang et al. (1993). Arrows mark transitions between L-type and class A sequence of the constructs indicated above the arrows (see also Figure 1A). Residues within the α_{1A} sequence not found in one of either DHP-sensitive α_1 subunits studied are highlighted. Asterisks indicate residues identical within all L-type and also identical within all ''non-L-type'' channels cloned so far, but different between L-type and non-L-type channels.

were identical within all L-type channels and also identical within all ''non-L-type'' channels cloned so far, but that were heterologous comparing L-type with non-L-type channels. These residues are clustered especially within transmembrane segments IIIS5 and IIIS6 and are major candidates for further mutational analyses. From the DHP insensitivity of chimeras AL1, AL2, AL6, AL11, AL14, and AL15, we conclude that residues in IIIS5, in the IIIS5-IIIS6 linker, and in IIIS6 are required for forming the DHP interaction site in repeat III. As previously shown, the sequence stretch between SS2 in repeat III and the N-terminal portion of IIIS6 (Figure 6) (chimera CBC3 by Tang et al., 1993) can be replaced by α_{1A} sequence without effect on DHP agonist and antagonist sensitivity. Therefore, amino acids determining DHP sensitivity in repeat III must be located between positions 1063–1144 and 1180–1197 (numbers refer to α_{1C}; Mikami et al., 1989).

Differential Interaction of DHP Agonists and Antagonists Within Repeat IV

In repeat IV, residues important for DHP agonist and antagonist action can be predicted more precisely. The sequence stretch supporting DHP antagonist sensitivity in chimera AL13 is indicated (Figures 1A, 5B, and 6). Accordingly, α_{1C} containing α_{1A} sequence in chimera CBC7 (see Figure 6) reported by Tang et al. (1993) supported DHP antagonist sensitivity. Thus, the crucial amino acids must reside between positions 1414 and 1450 (α_{1C}). This region includes a highly acidic 8 amino acid residue insert in α_{1A}, as well as 17 residues heterologous to our DHP-sensitive subunits.

Additional residues between positions 1454 and 1498 (α_{1C} numbering) are essential to create agonist (Bay K 8644) sensitivity. Concerning transmembrane segment IVS6, agonist sensitivity is restricted to 7 amino acid differences. As DHP agonists are believed to open the channel via formation of a hydrogen bond (Triggle et al., 1991), we consider tyrosine (1490) as the most likely interaction site (Figure 6).

The L-type sequence stretches important for DHP sensitivity (as outlined in Figure 5) include all regions that have been previously identified as parts of the DHP receptor domain of purified rabbit skeletal muscle α_1 subunits by photoaffinity labeling and antibody mapping (Nakayama et al., 1991; Striessnig et al., 1991). The importance of IIIS6 and the IIIS5-IIIS6 linker has been predicted from these studies. Moreover, photolabeling with the DHP antagonist (+)-[^{3}H]isradipine also predicted the minor importance of IVS6 for DHP antagonist interaction, a finding confirmed by our results. In contrast to an interpretation of a preliminary study (Tang et al., 1993), we consider antibody mapping analysis of photolabeled regions a very valuable tool to predict the positions of drug receptor sites within ion channel proteins. Mutational studies will mainly allow delineation of amino

acid residues involved in the binding of critical pharmacophores of drugs. Antibody mapping of photolabeled regions should also yield information about the localization of drug–protein interaction sites that contribute only weakly to binding affinity. Therefore, they provide helpful information about more peripheral portions of the DHP binding pocket and, thus, about the tertiary structure of α_1 subunits.

Together, our data substantially restrict the regions important for DHP interaction within L-type Ca^{2+} channel α_1 subunits. They pave the way for an even more detailed analysis of the DHP binding domain on the level of individual amino acid residues.

Experimental Procedures

Construction of Chimeric α_1 cDNAs

L-type α_1 chimeras L(h/s) and class A/L-type chimeras AL1-AL12(h/s) and AL13-AL15 (see Figure 1A) between the DHP-insensitive rabbit brain class A Ca^{2+} channel (BI-2) α_{1A} (A; Mori et al., 1991) and the DHP-sensitive L-type channels from carp skeletal muscle α_{1S} (S; Grabner et al., 1991) and rabbit heart $\alpha_{1C\text{-}a}$ (H; Mikami et al., 1989) were constructed and inserted into polyadenylating transcription plasmids pNKS2 (a gift of O. Pongs) or pSPCBI-2 (Mori et al., 1991) as follows.

Lh

Numbers in parentheses are amino acid numbers here and below, respectively: S(1–60), H(145–2171). The KpnI-AccIII fragment of H (5′ polylinker-620) (nucleotide numbers in parentheses here and below, respectively) was replaced by a KpnI-AccIII fragment of S (5′ polylinker-360) using a common AccIII restriction site of a KpnI-BamHI (5′ polylinker-1456) H subclone in pBluescript SK+ (Stratagene). This modification of the 5′ region leads to higher expression levels compared with unmodified $\alpha_{1C\text{-}a}$ cDNA and was therefore routinely used in our expression studies (Mitterdorfer et al., 1994, 1995; Wang et al., 1995).

To construct the following α_1 chimeras (as depicted in Figure 1A), PCR was used to create either common or compatible (SalI-XhoI; NsiI-PstI; XbaI-SpeI; HpaI-PvuII-EcoRV) restriction sites by introducing silent mutations (mutational sites indicated by an asterisk) or vast overlaps in using the ''gene SOEing'' technique (Horton et al., 1989). cDNA amplification by PCR (Thermocycler 60, Bio-Med) was performed with 35 cycles at low stringency (1 min at 94°C, 30 s at 42°C, 1.5 min at 72°C) using proofreading Pfu-polymerase (Stratagene).

Ls

S(1–60), H(145–920), S(806–1852). This chimera was assembled by ligating the BamHI-HindIII* fragment of H (1456–2953) together with a HindIII-XhoI fragment of S (2600–3′ polylinker) into the BamHI (1456H) and XhoI (6923H) sites of Lh.

Chimeric constructs AL1-AL15 were generated using carp skeletal muscle α_{1S} due to the more favorable location of (putative) restriction enzyme cleavage sites as compared with α_{1C}.

AL1

A(1–1406), S(965–1104), A(1544–1723), S(1311–1437), A(1856–2424). The ligation product from the NheI-PvuII fragment of A (3543–4512) plus the PvuII*-ClaI* fragment of S (3076–3498) was coligated with the ligation product from the ClaI*-NsiI* fragment of A (4925–5456) plus the PstI*-SphI* fragment of S (4107–4498) into the NheI (3543A) and SphI (5862A) sites of plasmid pSPCBI-2 after polylinker reduction.

AL2

S(1–60), H(145–920), A(1244–1406), S(965–1104), A(1544–1723), S(1311–1437), A(1856–2424). HindIII*-PvuII fragment of AL1 (4024A-4512A) was ligated together with PvuII*-BamHI fragment (partial cut) of AL1 (3076S-7615A) into the HindIII (2600S) and BamHI (3′ polylinker) sites (partial cut) of chimera Ls.

AL3

S(1–60), H(145–920), S(806–1104), A(1544–1723), S(1311–1437), A(1856–2424). KpnI-SalI fragment of Ls (5′ polylinker-3317S) was coligated with SalI-BamHI fragment of AL2 (3317S-3′ polylinker) into KpnI/BamHI polylinker sites of transcription plasmid pNKS2.

AL4

S(1–60), H(145–920), S(806–1104), A(1544–2424). ClaI*-SphI fragment of A (4925–5862) was coligated with an SphI-SpeI fragment of AL3 (5862A-3′ polylinker) into the ClaI* (4925A) and SpeI (3′ polylinker) sites of AL3.

AL5

S(1–60), H(145–422), A(348–724), H(794–920), S(806–1104), A(1544–1723), S(1311–1437), A(1856–2424). BamHI*-SpeI* fragment of A (1333–2464) was coligated with SpeI*-ClaI* fragment of AL3 (2569H-3498S) into the BamHI (1456H) and ClaI* (4925A) sites of AL3 after deletion of the BamHI site in the 3′ polylinker.

AL6

S(1–60), H(145–422), A(348–724), H(794–920), S(806–1034), A(1377–1723), S(1311–1437), A(1856–2424). SpeI*-SalI* fragment of AL5 (2569H-2984S) was coligated with the SalI*-ClaI* fragment of A (4420–4925) into the SpeI* (2464A) and ClaI* (4925A) sites of AL5.

AL7

S(1–60), H(145–422), A(348–1309), S(872–1104), A(1544–1723), S(1311–1437), A(1856–2424). XhoI-ApaI fragment of A (1689–3949) was coligated with the ligation product from the ApaI-NarI* fragment of A (3949–4220) plus the NarI*-SalI fragment of S (2796–3317) into the XhoI (1689A) and SalI (3317S) sites of AL5.

AL8

S(1–60), H(145–422), A(348–1369), S(928–1104), A(1544–1723), S(1311–1437), A(1856–2424). NheI-ClaI* fragment (3543A-3498S) was generated by gene SOEing (overlap: 4400A/2965S) and was inserted into the NheI (3543A) and ClaI* (4925A) sites of AL7.

AL9

A(1–1369), S(928–1104), A(1544–1723), S(1311–1437), A(1856–2424). HindIII-XhoI fragment of A in plasmid pSPCBI-2 (5′ polylinker-1679) was coligated with the XhoI-NheI fragment of A (1679–3543) into the HindIII (5′ polylinker) and NheI (3543A) sites of AL8.

AL10

A(1–1369), S(928–1104), A(1544–1723), S(1311–1376), A(1795–2424). ClaI*-XbaI* fragment of AL9 (4925A-4307S) was coligated with the SpeI*-BglII fragment of A (5671–6185) into the ClaI* (3498S) and BglII (6185A) sites of AL9.

AL11

A(1–1369), S(928–1046), A(1486–1723), S(1311–1376), A(1795–2424). SalI*-ClaI* fragment of A (4744–4925) was inserted into the SalI (3317S) and ClaI* (4925A) sites of AL10.

AL12s

A(1–1388), S(947–1082), A(1522–1723), S(1311–1402), A(1821–2424). The ligation product from the NheI-HpaI* fragment of A (3543–4464) plus the PvuII*-SalI fragment of S (3028–3317) was coligated with the ligation product from the SalI-HpaI* fragment of S (3317–3424) plus the EcoRV*-ClaI* fragment of A (4851–4925) into the NheI (3543A) and ClaI* (4925A) sites of AL9. This intermediate clone was modified by the following step: ClaI*-SpeI* fragment of AL9 (4925A-4409S) was coligated with the XbaI*-BglII fragment of A (5773–6185) into the ClaI* (4925A) and BglII (6185A) sites of the intermediate clone.

AL12h

A(1–1388), H(1062–1197), A(1522–1723), H(1413–1506), A(1821–2424). The ligation product from the NheI-HpaI* fragment of A (3543–4464) plus the EcoRV*-BglII fragment of H (3381–3704) was coligated with the ligation product from the BglII-HpaI* fragment of H (3704–3777) plus the EcoRV*-ClaI* fragment of A (4851–4925) into the NheI (3543A) and ClaI* (4925A) sites of AL9. The resulting intermediate clone was modified as follows: ligation product from the ClaI*-NsiI* fragment of A (4925–5456) plus the PstI*-SpeI* fragment of H (4421–4729) was coligated with XbaI*-SphI* fragment of A (5773–5862) into the ClaI* (4925A) and SphI (5862A) sites of the intermediate clone.

AL13

S(1–60), H(145–422), A(348–724), H(794–920), S(806–1104), A(1544–1723), S(1311–1352), A(1774–2424). ClaI*-NsiI* fragment of AL1 (4925A-4244S) was coligated with the NsiI*-BglII fragment of A (5617–6185) into the ClaI* (3498S) and BglII (6185A) sites of AL5.

AL14

A(1–1369), S(928–967), A(1409–1483), S(1045–1104), A(1544–1723), S(1311–1437), A(1856–2424). NheI-PvuII* fragment of AL9 (3543A-3076S) was coligated with the PvuII-SalI* fragment of A (4512–4744) into the NheI (3543A) and SalI (3317S) sites of AL9.

AL15
A(1–1369), S(928–1046), A(1486–1723), S(1311–1437), A(1856–2424). SalI*-ClaI* fragment of chimera AL11 (4744A-4925A) was inserted into the SalI (3317S) and ClaI* (4925A) sites of AL9.

Chimeric constructs were verified by extensive restriction enzyme mapping, by using at least two independent clones or by confirming their nucleotide composition by cDNA sequencing with the dideoxy chain termination method (Sanger et al., 1977).

Expression of α_1 Chimeras in X. laevis Oocytes
Capped run-off poly(A)$^+$ cRNA transcripts from XbaI linearized cDNA templates were synthesized (Krieg and Melton, 1984) and injected (15 ng/50 nl) into X. laevis oocytes (stage V-VI) together with approximately equimolar ratios of β_{1a} subunit cRNA (5 ng/50 nl; Ruth et al., 1989).

Two-microelectrode voltage-clamp recordings were carried out 2–5 days after injection and incubation of the oocytes at 19°C (Methfessel et al., 1986). Oocytes were prepared as previously described (Wang et al., 1995) and were analyzed for the presence of Ba^{2+} inward currents (I_{Ba}) through voltage-dependent Ca^{2+} channels using the conventional two microelectrode voltage-clamp technique (Turbo Tec 01C, NPI-Electronic, Germany). Voltage recording microelectrodes and current injecting electrodes were filled with 2.8 M CsCl, 0.2 M CsOH, 10 mM EGTA, 10 mM HEPES (pH 7.4) and had resistances of 0.3–1 MΩ. All experiments were carried out at room temperature using Ba^{2+} as the charge carrier in solutions composed of 40 mM $Ba(OH)_2$ or 2 mM $Ba(OH)_2$ (''high barium'' and ''low barium'' solution, respectively), 40 mM N-methyl-D-glucamine, 10 mM HEPES, and 10 mM glucose (pH adjusted to 7.4 with methanesulfonic acid). The recording chamber with a volume of 150 μl was continuously perfused with a flow rate of 1 ml/min; drug-containing solutions were applied with identical flow rate. Leakage current correction was performed either by subtracting the Cd^{2+}-sensitive current (10 μM Cd^{2+} added) or, digitally, by using average values of scaled leakage currents elicited by hyperpolarizing voltage pulses (P/6 protocol). The pClamp software package (vers. 5.51; Axon Instruments, Inc.) was used for data acquisition and analysis. Data were filtered at 1 kHz, digitized at 0.2 kHz, and stored on a computer hard disk.

Experiments with peptide toxins ω-Aga-IVA and ω-CTx-MVIIC were performed in low barium solutions as described (Sather et al., 1993). To ensure maximum expression of I_{Ba} under these experimental conditions, α_2/δ subunit cRNA (10 ng/50 nl; Ellis et al., 1988) was coinjected. ω-Aga-IVA was obtained from BioTrend (Cologne, Germany); synthetic ω-CTx-MVIIC, from Saxon Biochemicals (Hannover, Germany). Toxins were added from 0.1 or 1 mM stock solutions in distilled water. Unless stated otherwise, holding potential was −80 mV, and test potentials were applied to the peak of the I–V curve.

Acknowledgments

Correspondence should be addressed to M. G. We are grateful to Drs. Y. Mori and K. Imoto for the generous gift of the α_{1A} cDNA; to A. Schwartz for the $\alpha_{1C\text{-}a}$ and α_2/δ cDNAs; to O. Pongs for providing the transcription plasmid pNKS2; and to K. G. Beam for valuable comments on the manuscript. We would also like to thank Dr. J. Mitterdorfer for helpful discussions during the course of the project, Dr. V. E. Degtiar for experimental support, and F. Rosenthal and B. Kurka for expert technical assistance. This work was supported by grants from the Fonds zur Förderung der Wissenschaftlichen Forschung (S6601-med to H. G., S6602-med to J. S., and S6603-med to S. H.) and by the Dr. Legerlotz Stiftung.

The costs of publication of this article were defrayed in part by the payment of page charges. This article must therefore be hereby marked ''*advertisement*'' in accordance with 18 USC Section 1734 solely to indicate this fact.

Received August 30, 1995; revised October 2, 1995.

References

Bean, B.P. (1984). Nitrendipine block of cardiac calcium channels: high-affinity binding to the inactivated state. Proc. Natl. Acad. Sci. USA *82*, 6388–6392.

Bechem, M., and Hoffmann, H. (1993). The molecular-mode of action of the Ca^{2+} agonist (−)-Bay K 8644 on the cardiac Ca^{2+} channel. Pflügers Arch. *424*, 343–353.

Birnbaumer, L., Campbell, K.P., Catterall, W.A., Harpold, M.M., Hofmann, F., Horne, W.A., Mori, Y., Schwartz, A., Snutch, T.P., Tanabe, T., and Tsien, R.W. (1994). The naming of voltage-gated calcium channels. Neuron *13*, 505–506.

Catterall, W.A., and Striessnig, J. (1992). Receptor sites for calcium antagonists. Trends Pharmacol. Sci. *13*, 256–262.

Catterall, W.A., Seagar, M.J., and Takahashi, M. (1988). Molecular properties of dihydropyridine-sensitive calcium channels in skeletal muscle. J. Biol. Chem. *263*, 3535–3538.

De Lean, A., Munson, P.J., and Rodbard, D. (1978). Simultaneous analysis of families of simoid curves: application to bioassays, radioligand assay and physiological dose–response curves. Am. J. Physiol. *4*, 97–102.

Dunlap, K., Luebke, J.I., and Turner, T.J. (1995). Exocytotic Ca^{2+} channels in mammalian central neurons. Trends Neurosci. *18*, 89–98.

Ellinor, P.T., Zhang, J.F., Horne, W.A., and Tsien, R.W. (1994). Structural determinants of the blockade of N-type calcium channels by a peptide neurotoxin. Nature *372*, 272–275.

Ellis, S.B., Williams, M.E., Ways, N.R., Brenner, R., Sharp, A.H., Leung, A.T., Campbell, K.P., McKenna, E., Koch, W.J., Hui, A., et al. (1988). Sequence and expression of mRNAs encoding the α_1 and α_2 subunits of a DHP-sensitive calcium channel. Science *241*, 1661–1664.

Georgiadis, M.M., Komiya, H., Chakrabarti, P., Woo, D., Kornuc, J.J., and Rees, D.C. (1992). Crystallographic structure of the nitrogenase iron protein from *Azotobacter vinelandii*. Science *257*, 1653–1659.

Ginap, T., Dooley, D.J., and Feuerstein, T.J. (1993). The non-dihydropyridine L-type voltage-sensitive calcium channel activator FPL 64176 enhances K^+-evoked efflux of [^{3}H]norepinephrine from rat neocortical slices. Neurosci. Lett. *156*, 35–38.

Glossman, H., and Striessnig, J. (1990). Molecular properties of calcium channels. Rev. Physiol. Biochem. *114*, 1–105.

Grabner, M., Friedrich, K., Knaus, H.G., Striessnig, J., Scheffauer, F., Staudinger, R., Koch, W.J., Schwartz, A., and Glossmann, H. (1991). Calcium channels from *Cyprinus carpio* skeletal muscle. Proc. Natl. Acad. Sci. USA *88*, 727–731.

Grabner, M., Wang, Z., Mitterdorfer, J., Rosenthal, F., Charnet, P., Savchenko, A., Hering, S., Ren, D., Hall, L.M., and Glossmann, H. (1994). Cloning and functional expression of a neuronal calcium channel β subunit from house fly (*Musca domestica*). J. Biol. Chem. *269*, 23668–23674.

Gross, A., Abramson, T., and MacKinnon, R. (1994). Transfer of the scorpion toxin receptor to an insensitive potassium channel. Neuron *13*, 961–966.

Guy, H.R., and Conti, F. (1990). Pursuing the structure and function of voltage-gated channels. Trends Neurosci. *13*, 201–206.

Hering, S., Bolton, T.B., Beech, D.J., and Lim, S.P. (1989). Mechanism of calcium channel block by D600 in single smooth muscle cells from rabbit ear artery. Circ. Res. *64*, 928–936.

Hess, P. (1990). Calcium channels in vertebrate cells. Annu. Rev. Neurosci. *13*, 337–356.

Hess, P., Lansman, J.B., and Tsien, R.W. (1984). Different modes of Ca^{2+} channel gating behaviour favoured by dihydropyridine Ca^{2+} agonists and antagonists. Nature *311*, 538–544.

Hille, B. (1992). Calcium Channels. In Ionic Channels of Excitable Membranes, 2nd Ed., B. Hille, ed. (Sunderland, Massachusetts: Sinauer Associates, Inc.), pp. 83–114.

Hofmann, F., Biel, M., and Flockerzi, V. (1994). Molecular basis for Ca^{2+} channel diversity. Annu. Rev. Neurosci. *17*, 399–418.

Horton, R.M., Hunt, H.D., Ho, S.N., Pullen, J.K., and Pease, L.R. (1989). Engineering hybrid genes without the use of restriction enzymes: gene splicing by overlap extension. Gene *77*, 61–68.

Hughes, A.D., Hering, S., and Bolton, T.B. (1990). Evidence that agonist and antagonist enantiomers of the dihydropyridine PN202–

791 act at different sites on the voltage-dependent calcium channel of vascular muscle. Br. J. Pharmacol. *101*, 3–5.

Kamp, T.J., Sanguinetti, M.C., and Miller, R.J. (1989). Voltage- and use-dependent modulation of cardiac calcium channels by the dihydropyridine (+)-202–791. Circ. Res. *64*, 338–351.

Kass, R.S., and Arena, J.P. (1989). Influence of pH on calcium channel block by amlodipine, a charged dihydropyridine compound. J. Gen. Physiol. *93*, 1109–1127.

Kass, R.S., Arena, J.P., and Chin, S. (1991). Block of L-type calcium channels by charged dihydropyridines. J. Gen. Physiol. *98*, 63–75.

Krieg, P.A., and Melton, D.A. (1984). Functional messenger RNAs are produced by SP6 *in vitro* transcription of cloned cDNAs. Nucleic Acids Res. *12*, 7057–7070.

Kunze, D.L., and Rampe, D. (1992). Characterization of the effects of a new Ca^{2+} channel activator, FPL 64176, in GH3 cells. Mol. Pharmacol. *42*, 666–670.

Lacerda, A.E., and Brown, A.M. (1989). Nonmodal gating of cardiac calcium channels as revealed by dihydropyridines. J. Gen. Physiol. *93*, 1243–1273.

Lacerda, A.E., Kim, H.S., Ruth, P., Perez-Reyes, E., Flockerzi, V., Hofmann, F., Birnbaumer, L., and Brown, A.M. (1991). Normalization of current kinetics by interaction between the α_1 and β subunits of the skeletal muscle dihydropyridine-sensitive calcium channel. Nature *352*, 527–530.

Marks, T.N., and Jones, S.W. (1992). Calcium currents in the A7r5 smooth muscle–derived cell line. J. Gen. Physiol. *99*, 367–390.

Methfessel, C., Witzemann, V., Takahashi, T., Mishina, M., Numa, S., and Sakmann, B. (1986). Patch clamp measurements on *Xenopus laevis* oocytes: currents through endogenous channels and implanted acetylcholine receptor and sodium channels. Pflügers Arch. *407*, 577–588.

Mikami, A., Imoto, K., Tanabe, T., Niidome, T., Mori, Y., Takeshima, H., Narumiya, S., and Numa, S. (1989). Primary structure and functional expression of the cardiac dihydropyridine-sensitive calcium channel. Nature *340*, 230–233.

Mitterdorfer, J., Froschmayr, M., Grabner, M., Striessnig, J., and Glossmann, H. (1994). Calcium channels: the β-subunit increases the affinity of dihydropyridine and Ca^{2+} binding sites of the α_1-subunit. FEBS Lett. *352*, 141–145.

Mitterdorfer, J., Sinnegger, M.J., Grabner, M., Striessnig, J., and Glossmann, H. (1995). Coordination of Ca^{2+} by the pore region glutamates is essential for high affinity dihydropyridine binding to the cardiac Ca^{2+} channel α_1 subunit. Biochemistry *34*, 9350–9355.

Mori, Y., Friedrich, T., Kim, M.-S., Mikami, A., Nakai, J., Ruth, P., Bosse, E., Hofmann, F., Flockerzi, V., Furuichi, T., et al. (1991). Primary structure and functional expression from complementary DNA of a brain calcium channel. Nature *350*, 398–402.

Nakai, J., Adams, B.A., Imoto, K., and Beam, K.G. (1994). Critical roles of the S3 segment and S3-S4 linker of repeat I in activation of L-type calcium channels. Proc. Natl. Acad. Sci. USA *91*, 1014–1018.

Nakayama, H., Taki, M., Striessnig, J., Glossmann, H., Catterall, W.A., and Kanaoka, Y. (1991). Identification of 1,4-dihydropyridine binding regions within the α_1 subunit of skeletal muscle calcium channels by photoaffinity labeling. Proc. Natl. Acad. Sci. USA *88*, 9203–9207.

Ragsdale, D.S., McPhee, J.C., Scheuer, T., and Catterall, W.A. (1994). Molecular determinants of state-dependent block of Na^+ channels by local anesthetics. Science *265*, 1724–1728.

Randall, A., and Tsien, R.W. (1995). Pharmacological dissection of multiple types of Ca^{2+} channel currents in rat cerebellar granule neurons. J. Neurosci. *15*, 2995–3012.

Ruth, P., Roehrkasten, A., Biel, M., Bosse, E., Regulla, S., Meyer, H.E., Flockerzi, V., and Hofmann, F. (1989). Primary structure of the β subunit of the DHP-sensitive calcium channel from skeletal muscle. Science *245*, 1115–1118.

Sanger, F., Nicklen, S., and Coulson, A.R. (1977). DNA sequencing with chain-terminating inhibitors. Proc. Natl. Acad. Sci. USA *74*, 5463–5467.

Sanguinetti, M.C., Krafte, D.S., and Kass, R.S. (1986). Voltage-dependent modulation of Ca^{2+} channel current in heart cells by Bay K 8644. J. Gen. Physiol. *88*, 369–392.

Sather, W.A., Tanabe, T., Zhang, J.-F., Mori, Y., Adams, M.E., and Tsien, R.W. (1993). Distinctive biophysical and pharmacological properties of class A (BI) calcium channel α_1 subunits. Neuron *11*, 291–303.

Sprang, S., Goldsmith, E., and Fletterick, R. (1987). Structure of the nucleotide activation switch in glycogen phosphorylase a. Science *237*, 1012–1019.

Stea, A., Tomlinson, W.J., Soong, T.W., Bourinet, E., Dubel, S.J., Vincent, S.R., and Snutch, T.P. (1994). Localization and functional properties of a rat brain α_{1A} calcium channel reflect similarities to neuronal Q-type and P-type channels. Proc. Natl. Acad. Sci. USA *91*, 10576–10580.

Striessnig, J., Murphy, B.J., and Catterall, W.A. (1991). Dihydropyridine receptor of L-type Ca^{2+}-channels: Identification of binding domains for [^{3}H](+)-PN200–110 and [^{3}H]azidopine within the α_1 subunit. Proc. Natl. Acad. Sci. USA *88*, 10769–10773.

Strübing, C., Hering, S., and Glossmann, H. (1993). Evidence for an external location of the dihydropyridine agonist receptor site on smooth muscle and skeletal muscle calcium channels. Br. J. Pharmacol. *108*, 884–891.

Tanabe, T., Takeshima, H., Mikami, A., Flockerzi, V., Takahashi, H., Kangawa, K., Kojima, M., Matsuo, H., Hirose, T., and Numa, S. (1987). Primary structure of the receptor for calcium channel blocker from skeletal muscle. Nature *328*, 313–318.

Tanabe, T., Adams, B.A., Numa, S., and Beam, K.G. (1991). Repeat I of the dihydropyridine receptor is critical in determining calcium channel activation kinetics. Nature *352*, 800–803.

Tang, S., Yatani, A., Bahinski, A., Mori, Y., and Schwartz, A. (1993). Molecular localization of regions in the L-type calcium channel critical for dihydropyridine action. Neuron *11*, 1013–1021.

Triggle, D.J., Hawthorn, M., Gopalakrishnan, M., Minarini, A., Avery, S., Rutledge, A., Bangalore R., and Zheng, W. (1991). Synthetic organic ligands active at voltage-gated calcium channels. Ann. NY Acad. Sci. *635*, 123–138.

Varadi, G., Lory, P., Schultz, D., Varadi, M., and Schwartz, A. (1991). Acceleration of activation and inactivation by the β subunit of the skeletal muscle calcium channel. Nature *352*, 159–162.

Wang, Z., Grabner, M., Berjukov, S., Savchenko, A., Glossmann, H., and Hering, S. (1995). Chimeric L-type calcium channels expressed in *Xenopus laevis* oocytes reveal role of repeats III and IV in activation gating. J. Physiol. *486.1*, 131–137.

Wei, X., Perez-Reyes, E., Lacerda, A.E., Schuster, G., Brown, A.M., and Birnbaumer, L. (1991). Heterologous regulation of the cardiac Ca^{2+} channel α_1 subunit by skeletal muscle β and γ subunits. Implications for the structure of cardiac L-type Ca^{2+} channels. J. Biol. Chem. *266*, 21943–21947.

Wheeler, D.B., Randall, A., and Tsien, R.W. (1994). Roles of N-type and Q-type Ca^{2+} channels in supporting hippocampal synaptic transmission. Science *264*, 107–111.

Zhang, J.F., Ellinor, P.T., Aldrich, R.W., and Tsien, R.W. (1994). Molecular determinants of voltage-dependent inactivation in calcium channels. Nature *372*, 97–100.